Solar Physics
DOI: 10.1007/•••••-•••-•••-••••-•

Long- and Mid-Term Variations of the Soft X-ray Flare Type in Solar Cycles

I.M. Chertok[1] · **A.V. Belov**[1]

Received ; accepted

Abstract
Using data from the *Geostationary Operational Environmental Satellites* (GOES) spacecraft in the 1 – 8 Å wavelength range for Solar Cycles 23, 24, and part of Cycles 21 and 22, we compare mean temporal parameters (rising, decay times, duration) and the proportion of impulsive short-duration events (SDE) and gradual long-duration events (LDE) among C- and ≥M1.0-class flares. It is found that the fraction of the SDE ≥M1.0-class flares (including spikes) in Cycle 24 exceeds that in Cycle 23 in all three temporal parameters at the maximum phase and in the decay time during the ascending cycle phase. However, Cycles 23 and 24 barely differ in the fraction of the SDE C-class flares. The temporal parameters of SDEs, their fraction, and consequently the relationship between the SDE and LDE flares do not remain constant, but they reveal regular changes within individual cycles and during the transition from one cycle to another. In all phases of all four cycles, these changes have the character of pronounced, large-amplitude "quasi-biennial" oscillations (QBOs). In different cycles and at the separate phases of individual cycles, such QBOs are superimposed on various systematic trends displayed by the analyzed temporal flare parameters. In ycle 24, the fraction of the SDE ≥M1.0-class flares from the N- and S-hemispheres displays the most pronounced synchronous QBOs. The QBO amplitude and general variability of the intense ≥M1.0-class flares almost always markedly exceeds those of the moderate C-class flares. The ordered quantitative and qualitative variations of the flare type revealed in the course of the solar cycles are discussed within the framework of the concept that the SDE flares are associated mainly with small sunspots (including those in developed active regions) and that small and large sunspots behave differently during cycles and form two distinct populations.

Keywords: Short-term flares; Long-duration flares; Quasi-biennial oscillations; Solar cycles

[1]Pushkov Institute of Terrestrial Magnetism, Ionosphere and Radio Wave Propagation (IZMIRAN), Troitsk, Moscow, 108840 Russia, email: ichertok@izmiran.ru; abelov@izmiran.ru

1. Introduction

Solar flares are very diverse in many of their features, characteristics, and parameters (see, *e.g.*, Fletcher *et al.*, 2011 for a review). For example, in the soft X-ray range, two extreme varieties of the flares are distinguished from the viewpoint of their temporal profiles. Figure 1a illustrates an example of these extreme varieties observed by the *Geostationary Operational Environmental Satellites* (GOES: Bornmann *et al.*, 1996). In this case, on 20 August 1999, a gradual long-duration (LDE) M1.8-class flare occurred at first and then in the interval of a few hours a very short-duration, impulsive, more intense M9.8-class flare took place in the same active region. For convenience and by analogy with LDEs, we will refer to such and similar flares as short-duration events (SDEs). The characteristic time of LDEs is many hours, in that the decay time significantly exceeds the rise time. Therefore, the LDE abbreviation is often treated as Long-Decay Events (Kahler, 1977). On the other hand, the extremely impulsive flares last a few minutes only and have a symmetric temporal profile with approximately equally short rise and decay times without additional descending behavior. On the standard GOES three-day plots (such as Figure 1a) such SDEs look like spikes. Of course, there are many flares of intermediate character or so-called hybrid flares in which the LDE and impulsive components are observed in various combinations (Švestka, 1989; Tomczak and Dubieniecki, 2015). Many LDE flares start with an impulsive phase. As for extreme spike flares, they may occur not only separately but also at the initial phase of combined flares and during any stage of weaker background LDEs.

It is known (Pallavicini, Serio, and Vaiana, 1977; Ohki *et al.*, 1983; Švestka, 1989) that the SDE flares are generated in isolated, compact (confined) sources as a result of the local reconnection of small-scale magnetic structures (loops) very low over active regions (ARs). The short-duration of impulsive flares is due to the fact that in them the compact energy release is followed by rapid conductive cooling. Such flares are usually accompanied by collimated jets, which sometimes can transform into narrow coronal mass ejections (CMEs). The main distinctive features of the LDE flares result from the presence of large CMEs and long-duration post-eruptive energy release that they cause. At this phase, the active region magnetosphere, strongly disturbed by a CME, relaxes to the initial state by means of the reconnection in a long, vertical current sheet that provides prolonged additional energy release. This is accompanied by the formation of more and more new high loops, composing a coronal arcade with diverging two flare ribbons at their footpoints. Because of these properties, LDEs are often referred to as eruptive or two-ribbon flares (Janvier, Aulanier, and Démoulin, 2015; Zuccarello *et al.*, 2017). Thus, unlike SDEs, which have mainly a local character, LDEs span practically the entire magnetosphere over an AR. This can be seen in the example of the flares on 20 August 1999 mentioned above. As the 195 Å *Solar and Heliospheric Observatory/Extreme ultraviolet Imaging Telescope* (SOHO/EIT) images (Figure 1b) show, the LDE flare was accompanied by a large-scale arcade and the spike flare initiated from a small compact source located outside the LDE flare ribbon.

Quite often the intense SDE or LDE flares occur in series, when within a few days one AR produces mainly uniform short-duration spike-like flares and

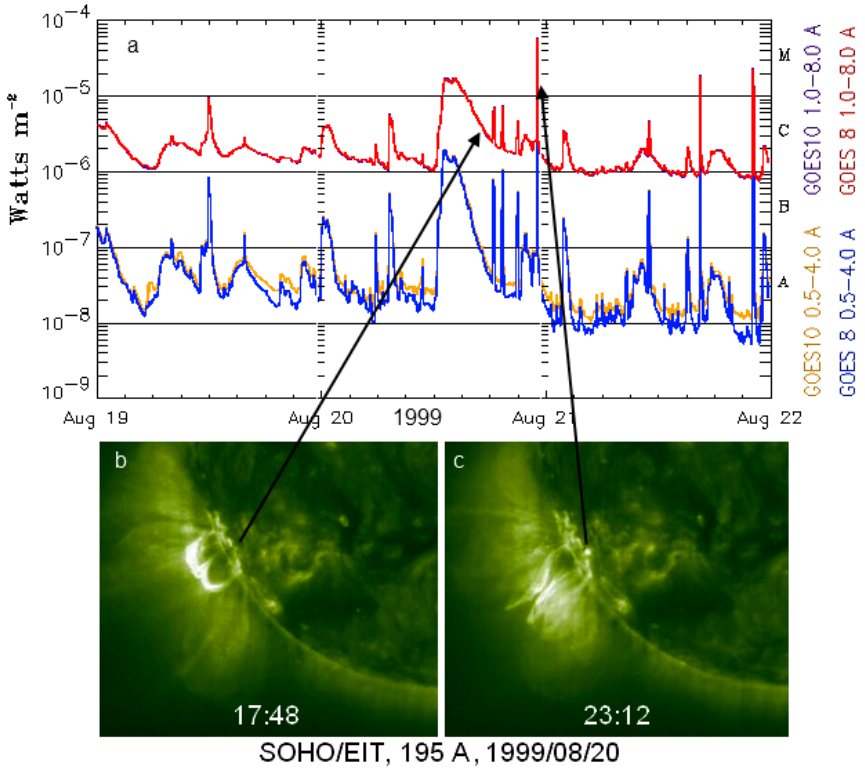

Figure 1. (a) The GOES soft X-ray three-day plot illustrating the gradual LDE and impulsive SDE (spike) M-class flares of 20 August 1999. (b, c) The SOHO/EIT 195 Å images displaying a post-eruptive arcade at the decay phase of the LDE flare and the compact source of the spike flare.

another AR generates predominantly homologous, gradual, long-duration flares. For example, according to the GOES soft X-ray data, a series of four very similar SDEs of the M- and X-class occurred on 6 – 8 September 2011 in AR11283 and seven similar LDEs of the same classes originated in AR11429 during the period of 2 – 13 March 2012 (see Figures 1s and 2s at the site www.izmiran.ru/~ichertok/FlareVariations/). It is obvious that such a sequence of flare activity is caused by peculiarities of the magnetic structure of the corresponding ARs, which remain able for several days to produce a local low-altitude reconnection in some cases and an extensive energy release with a developed post-eruptive phase in others.

Parameters of sunspots, characteristics of ARs, and solar activity as a whole strongly change in the course of the 11-year cycles (see a review of Hathaway, 2015). This stimulated us to study the cycling variations of the relationship between the SDE and LDE flares, *i.e.* changes of the flare character during the recent solar cycles. An additional cause for such an analysis arose from our impression formed in a result of many-years work with the GOES soft X-ray plots, that in the current weaker Cycle 24 the fraction of the impulsive flares (including spikes) is noticeably higher in comparison with Cycle 23. In the present article, we address two issues: i) comparison of the cycles by the

occurrence rate and trends of the SDE and LDE flares, which means long-term variations; ii) an analysis of the mid-term variations of the flare character during specific cycles. The structure of the article is as follows: The GOES data and analyzed parameters are described in Section 2. Subsection 3.1 is devoted to a study of histograms showing the fraction of intense and moderate SDE flares at the distinct phases of Cycles 23 and 24. In Subsection 3.2, we present the results of a more detailed analysis revealing the presence of stable, high-amplitude, antiphased quasi-biennial variations of the fraction of the SDE and LDE flares in Cycles 23, 24, and parts of in Cycles 21 and 22. In Section 4, we summarize the results and speculate that the qualitative variations of the flare character can be associated with the corresponding changes in magnetic features of sunspots and ARs in different solar cycles caused by features of the dynamo processes.

2. Data and Parameters

The GOES spacecraft have provided continuous solar monitoring for more than 40 years, in particular, in the soft X-ray 0.5 – 4 Å and 1 – 8 Å wavelength ranges. These data are published by the U.S. National Oceanic and Atmospheric Administration (NOAA), Space Weather Prediction Center (SWPC) as the three-day plots and the flare lists indicating their coordinates, class as well as the starting, maximum, and ending times. (See ftp://ftp.sec.noaa.gov/pub/warehouse/; ftp://ftp.ngdc.noaa.gov/STP/space-weather/solar-data/solar-features/solar-flares/x-rays/goes/xrs/, and Solar-Geophysical Data comprehensive and Weekly reports (ftp://ftp.ngdc.noaa.gov/STP/SOLAR_DATA/SGD_PDFversion/)). In our analysis, we deal with just these temporal parameters which have been included in the IZMIRAN Database (Belov *et al.*, 2005), in conjunction with many other solar and solar-terrestrial data. This database has allowed us to analyze the temporal characteristics of the soft X-ray flares of Cycles 21 – 24 in various combinations and representations.

According to the NOAA user guide (http://www.swpc.noaa.gov/sites/default/files/images/u2/Usr_guide.pdf), the start of an X-ray flare is defined as the first minute in a sequence of four minutes of steep monotonic increase in 1 – 8 Å flux. The time of the flare maximum is defined as the minute of the peak one-minute averaged value X-ray flux. The end time is the time when the flux level decays to a point halfway (half peak) between the maximum flux and the pre-flare background level. In comparing the SDE and LDE flares we are interested in their rising, decay times, and duration. It is clear that the rising time $[dt1]$ is calculated as an interval between moments of the flare start and maximum, and the decay time $[dt2]$ should be equal to the difference between the maximum and end times. Unfortunately, we are forced to accept that the flare end is determined by the flux reduction to the half-peak level. It is understood, that differences between the SDE and LDE flares would be much more obvious if the level one- tenth, for example, were to be used instead. In such a criterion, the decay time and duration, determined as $dt = dt1 + dt2$, would increase to a small degree for the SDE flares, but significantly for LDEs. Nevertheless, henceforward we will proceed from the original GOES tabular data.

We consider the sufficiently intense soft X-ray flares dividing them into two groups: i) flares of a moderate intensity with importance from C1.0 to C9.9 and ii) the most powerful flares of the ≥M1.0-class, including X-class flares. The reason is that the long- and medium-term variations of these intense flares can be most apparent and the peculiarities of their variations in the cycles are of most interest. Moreover, their temporal parameters, analyzed here, are not distorted in practice by the level of the background radiation, even at the maximum phase of the activity cycle.

The analysis shows (see Subsection 3.1.) that among these flares, those can be considered as impulsive or more generally as SDE ones, which have either a sufficiently rapid rise ($dt1 < 10$ minutes) and decay ($dt2 < 10$ minutes), or a short duration ($dt < 15$ minutes). Below we will discuss mainly such SDE flares. In some cases they will be contrasted with long-duration flares, having particularly those with a duration $dt2 > 30$ minutes which we consider as LDEs.

3. Analysis and Results

3.1. Temporal Histograms of Flares in Cycles 23 and 24

First of all, let us compare the distributions of the flares by their main temporal parameters in Cycles 23 and 24. We have divided each of these cycles into three phases. For Cycles 23 and 24, respectively, the ascending phases covered during 1997 – 1999 and 2010 – 2011, the maximum phases included 2000 – 2002.5 and 2012 – 2014.5, and the declining phases covered 2002.6 – 2007 and 2014.6 – 2016. In each of the two cycles at these phases, the number of flares of the C1.0 – C9.9 classes are measured in thousands and of the ≥M1.0-classes amounted to hundreds (see the N columns in Table 1). It should be added that the number of events at the indicated phases of Cycle 23 was more than that in Cycle 24 by factors 1.5 – 2.6 for the C-class flares and factors 2.3 – 2.5 for the ≥M1.0-class flares.

We have constructed histograms characterizing the relative distributions of the flare numbers at the three phases of Cycles 23 and 24 according to the flare temporal parameters. Figure 2 presents one set of such histograms relating to the decay time [$dt2$]. Here the green and orange bins belong to events of Cycles 23 and 24, and the left and right rows display the C- and the ≥M1.0-class flares, respectively. It can be seen that at all three phases of the both cycles and for two groups of flares, the histograms are fairly similar, particularly, in the sense that flares with the decay time $dt2 \approx 5 - 10$ minutes are observed most often. However, the percentage (fraction) of the SDE flares with $dt2 < 10$ minutes displays some interesting peculiarities. On the one hand, fractions of the SDE moderate C-class flares with $dt2 < 10$ minutes are nearly equal at the corresponding phases of Cycles 23 and 24: they differ by no more than 5 %. On the other hand, significant differences are visible in the powerful SDE ≥M1.0-class flares. The fractions of these flares at the ascending and maximum phases of Cycle 24 exceed the same fractions in Cycle 23 by more than 10 %. It is noteworthy that at the maximum phases such an excess of the fraction of the ≥M1.0-class occurs due to the most SDE flares with $dt2 < 5$ minutes.

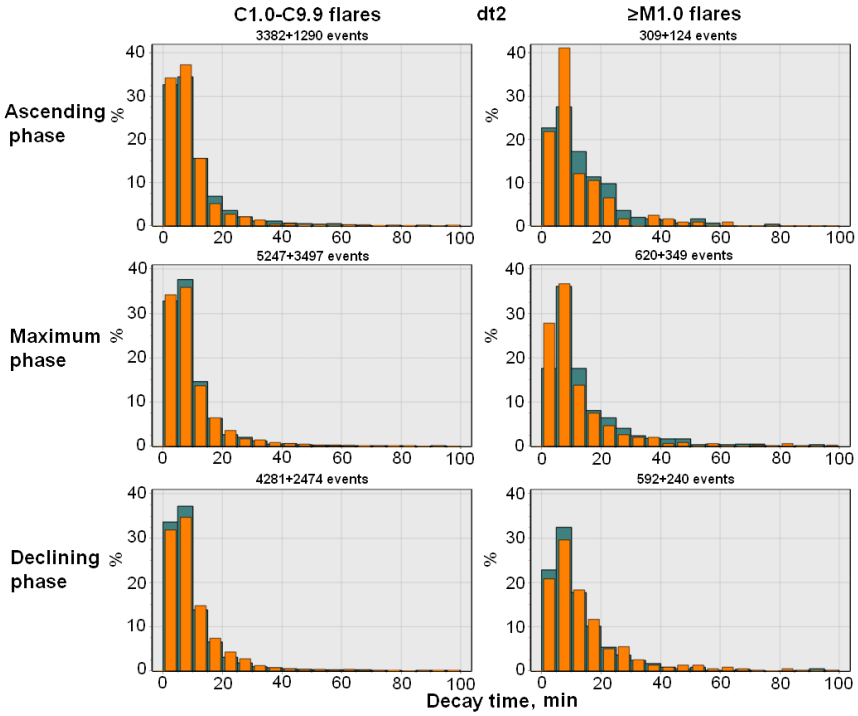

Figure 2. Relative distributions (percent) of the moderate C1.0 – C9.9 class flares (*left*) and the most intense ≥M1.0-class flares (*right*) by the decay time [*dt*2] at the ascending, maximum and declining phases of the Cycles 23 (*green*) and 24 (*orange*.

The analogous histograms have been constructed for two other temporal parameters: rising [*dt*1] and duration [*dt*]. For brevity, they are only presented at the site mentioned above www.izmiran.ru/~ichertok/FlareVariations/. The results of comparison of the occurrence of the SDE flares for all three parameters, including the described decay time [*dt*2], are summarized in Table 1. They confirm that Cycles 23 and 24 do not differ in the fraction of the SDE C-class flares. By the parameters *dt*1 and *dt*, this difference is within 2 %. At the same time, for the ≥M1.0-class flares and these parameters, a significant excess (>10 %) of fraction of SDEs in Cycle 24 in comparison with Cycle 23 is found, but at the maximum phase only.

In general, the data presented in Table 1 allow us to conclude that the relative number of the SDE ≥M1.0-class flares in Cycle 24 exceeds that in Cycle 23 for all three temporal parameters during the maximum phase and for the decay parameter [*dt*2] during the ascending phase (see the bold numbers). Thus, this corresponds to our preliminary impression resulting from the visual inspection of the numerous GOES soft X-ray plots.

3.2. Quasi-Biennial Variations and Trends

The results of the previous subsection motivated us to a more detailed analysis. We studied further the variations of the soft X-ray flare characteristics by

Table 1. The number [N] and percentage of the SDE C1.0 – C9.9 and ≥M1.0 flares with $dt1$ and $dt2$ <10 minutes, dt <15 minutes at the ascending, maximum, and declining phases of Cycles 23/24.

Cycle phase	C1.0 – C9.9 flares				≥M1.0 flares			
	N	$dt1$	$dt2$ [%]	dt	N	$dt1$	$dt2$ [%]	dt
Ascending	3382/1290	67/67	66/71	53/54	309/124	42/40	50/**62**	33/33
Maximum	5247/3497	70/70	70/70	55/55	820/349	43/**55**	53/**64**	33/**45**
Declining	4281/2474	65/63	70/65	51/49	820/349	40/38	55/51	31/33

averaging them within the running windows of ±one Carrington rotation with a step of two rotations. Near the minimum phases of the solar cycles, where the number of the C- and ≥M1.0-class flares is small, we kept for statistical significance only windows with $N > 10$. First, consider the variations of a number of the flare parameters during Cycles 23 and 24 shown in Figure 3 against the background of the NOAA monthly sunspot number (SSN)(www.ngdc.noaa.gov/stp/solar/ssndata.html).

Figure 3a demonstrates variations of the average decay time [$dt2$]. The first unexpected thing is the conspicuous, very pronounced, and regular quasi-periodic variations. Their characteristic temporal ranges roughly from 0.8 to 1.9 year. Sometimes it seems to be close to the so-called Rieger-type periodicity around of 154 days, which was detected in the occurrence rate of hard-emission flares during Cycle 21 (Rieger *et al.*, 1984). Nevertheless, following the accepted terminology (see Bazilevskaya *et al.*, 2014; Broomhall and Nakariakov, 2015), we will call these mid-term variations as "quasi-biennial" oscillations (QBOs). They are observed in flares of the both C- and ≥M1.0-classes almost completely during Cycle 23 and 24 and have rather large amplitude, reaching 35 – 40 % of the average value. Additionally it is noteworthy that the QBO amplitude of the most intense ≥M1.0-class flares is almost always several times larger than that of the moderate C-class flares. Only at the beginning and end of Cycle 23 does the QBO amplitude of the C-class flares increase to the level of the ≥M1.0-class flares. Generally the QBO amplitude of the average decay time $dt2$ appears to be larger than the amplitude of its long-term changes during both of the cycles. For most of the two cycles, the C- and ≥M1.0-class flares display almost synchronous variations, although sometimes this synchronism is interrupted, as happened for example around 1998 and 2013. QBOs behave somewhat differently in the two cycles. In Cycle 23, they are more pronounced than in Cycle 24. Moreover, the average value of $dt2$, particularly of the ≥M1.0-class flares in Cycle 24 (12.4±0.5 minutes), is somewhat less than that in Cycle 23 (13.8±0.4 minutes). The $dt2$-parameter decreases noticeably upon transition from Cycle 23 to Cycle 24 and reaches the smallest values at the beginning of the ascending phase of Cycle 24. During the high-activity period of Cycle 23 (1998 – 2005), QBOs are observed on the background of a downward trend of the $dt2$-parameter while signs of an upward trend of this parameter take place in Cycle 24.

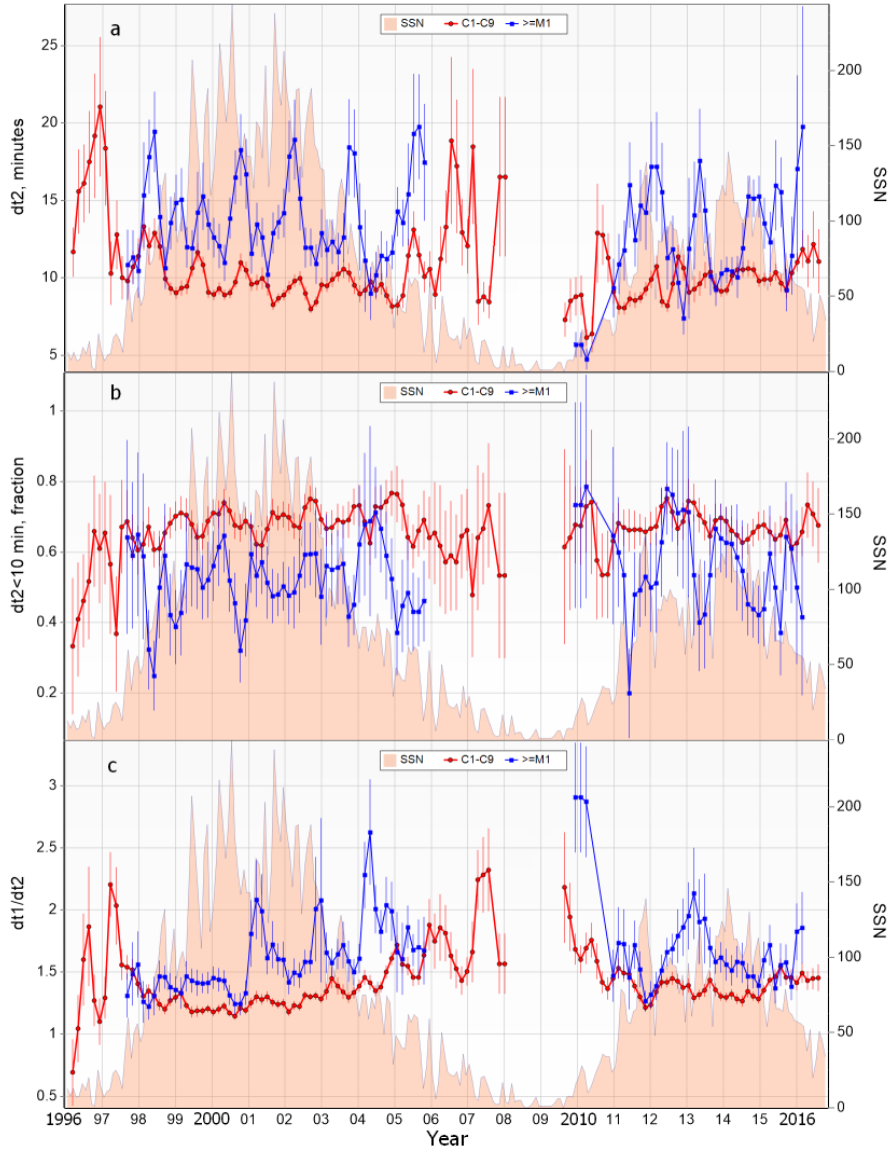

Figure 3. Variations of some parameters of the C-class (*red lines and circles*) and ≥M1.0-class (*blue lines and squares*) flares against the background of the monthly sunspot number (SSN) during Cycles 23 and 24: (a) the average decay time [$dt2$]; (b) fraction of the SDE flares with $dt2$ <10 minutes; (c) ratio of the rise and decay times [$dt1/dt2$]. Here and below the vertical line segments show $\pm 1\sigma$ standard deviations.

Figure 3b shows that QBOs of the average decay time [$dt2$] described above are caused by the corresponding quasi-biennial variations of the fraction of the SDE flares with $dt2$ <10 minutes. Comparison of Figures 3a and 3b shows that the $dt2$-value increases (decreases) when the fraction of SDEs decreases (rises). In particular, the fraction of the SDE flares is especially increased at the beginning of Cycle 24, and especially for the intense ≥M1.0-class flares. At the same time, the SDE fraction of the intense ≥M1.0-class flares is significantly reduced in both of the cycles during their ascending phases and during the Gnevyshev gaps between two SSN maximums of each cycle.

It is also interesting to consider variations of the ratio between the rise and decay times [$dt1/dt2$] (Figure 3c). This parameter also reveals QBOs, especially pronounced during the second half of Cycle 23. During the same part of this cycle, both the C- and ≥M1.0-class flares display an increasing trend of the $dt1/dt2$- parameter, while the opposite falling trend seems to be present during the first two years of Cycle 24 . The ratio $dt1/dt2$ is greatly increased at the beginning of Cycle 24 for the ≥M1.0-class flares, apparently because at this stage the average decay time $dt2$ was especially low for these flares (see Figure 3a). The same increase of $dt1/dt2$ is observed for the C-class flares, but to a lesser extent.

The main feature of the revealed variations outlined above is that the relationship between the SDE and LDE flares varies in a regular manner during cycles in the form of QBOs. This can be seen in Figure 4 where the fractions of SDEs with duration dt <15 minutes and LDEs with dt >30 minutes are compared for the ≥M1.0-class (a) and and C-class (b) flares. Among the ≥M1.0-class flares, the fraction of such SDEs and LDEs is about the same but with some predominance of LDEs in Cycle 23 and an opposite prevalence of the SDE flares in Cycle 24. Among the C-class (b) flares, SDEs are obviously dominant. As might be expected, the relationship between SDEs and LDEs varies inversely. For the ≥M1.0-class flares, opposite tendencies are observed in Cycles 23 and 24: the fraction of LDEs is increased at the onset and at the end of Cycle 23, while the fraction of SDEs is the largest after the first maximum and at the declining phase of Cycle 24. The most distinct antiphased variations of the SDE and LDE fractions took place near the first maximums and at the declining phases of the two cycles. For the C-class flares, again the SDE and LDE variability and their out-of-phase behavior is less pronounced than for the ≥M1.0-class flares.

Now consider in Figure 5 the fraction of the SDE ≥M1.0- (a) and C-class (b) flares with the duration dt <15 minutes occurred separately in the north (*solid line*) and south (*dashed line*) hemispheres. One can see that the clear QBOs are also observed in this case during both Cycles 23 and 24. However, the oscillations in Cycle 24 are much more pronounced than in Cycle 23, especially for the intense ≥M1.0-class flares in comparison with the moderate C-class flares. The maximum amplitude of QBOs, reaching 85 %, is observed in the powerful ≥M1.0-class flares of the N-hemisphere near the first maximum of the Cycle 24 in 2012. The fraction of the SDE ≥M1.0-class flares decreases to the minimum values near the Gnevyshev gaps of the both cycles and additionally at the onset of the declining phase of Cycle 24. In general, the fractional variations of the SDE ≥M1.0- and C- class flares do not coincide in time. Another remarkable feature

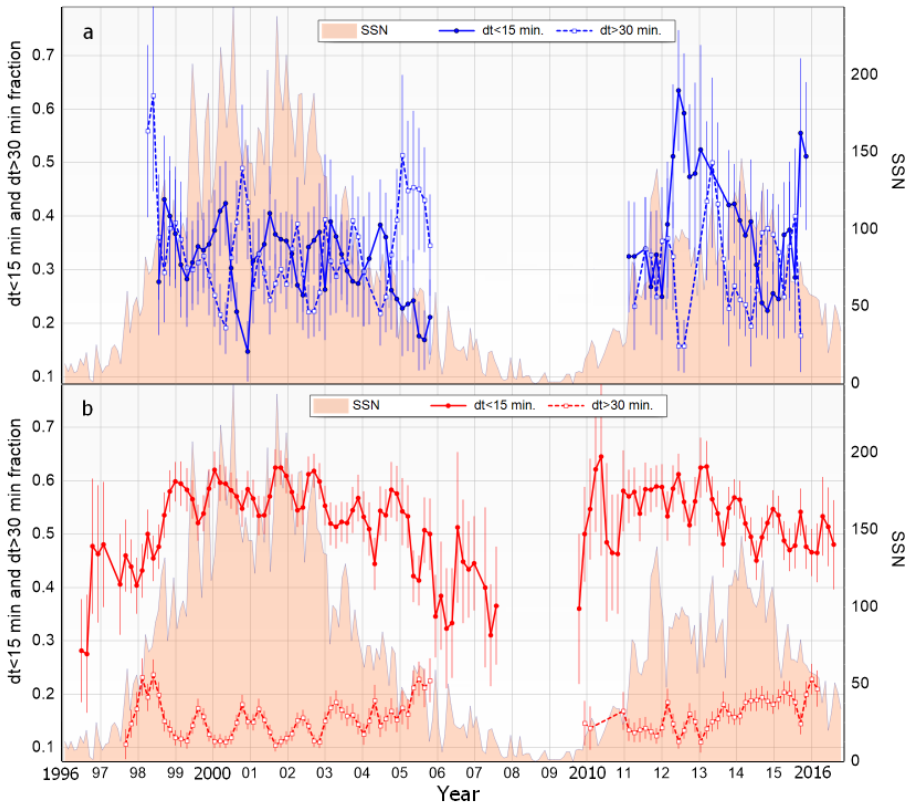

Figure 4. Fraction of SDEs (*solid lines*) with duration dt <15 minutes and LDEs (*dashed lines*) with dt >30 minutes among the ≥M1.0- (a) and C-class (b) flares in Cycles 23 and 24.

of Cycle 24 is a rather high synchronicity of the fractional QBOs of the SDE ≥M1.0-class flares from the N- and S-hemispheres. In Cycle 23, the similar synchronicity is observed only near the first maximum and Gnevyshev gap. At the ascending and declining phases of Cycle 23, the fraction of the SDE ≥M1.0-class flares from the N- and S-hemispheres display mainly antiphased variations. The intermittent synchronous and antiphased hemispherical fractional oscillations are characteristic of the SDE C-flares flares of both Cycles 23 and 24.

After a detailed consideration of Cycles 23 and 24, now it is reasonable to involve data of the previous Cycles 21 and 22, covering the period of 1977–1985 and 1987–1995 (Figure 6). However, here we confined ourselves to the rise temporal parameter [$dt1$] because there is no certainty that the decay time [$dt2$] and consequently duration [dt] were determined in these years by the same criteria as in Cycles 23 and 24.

From Figure 6a, on which variations of the average rise time [$dt1$] of the soft X-ray flares are presented, it follows that QBOs are characteristic not only of Cycles 23 and 24, but also of Cycles 21 and 22. In all four cycles, the QBO amplitude of the strongest ≥M1.0-class flares considerably exceeds that of the moderate C-class flares. Among other features, it is important to pay attention to the growing

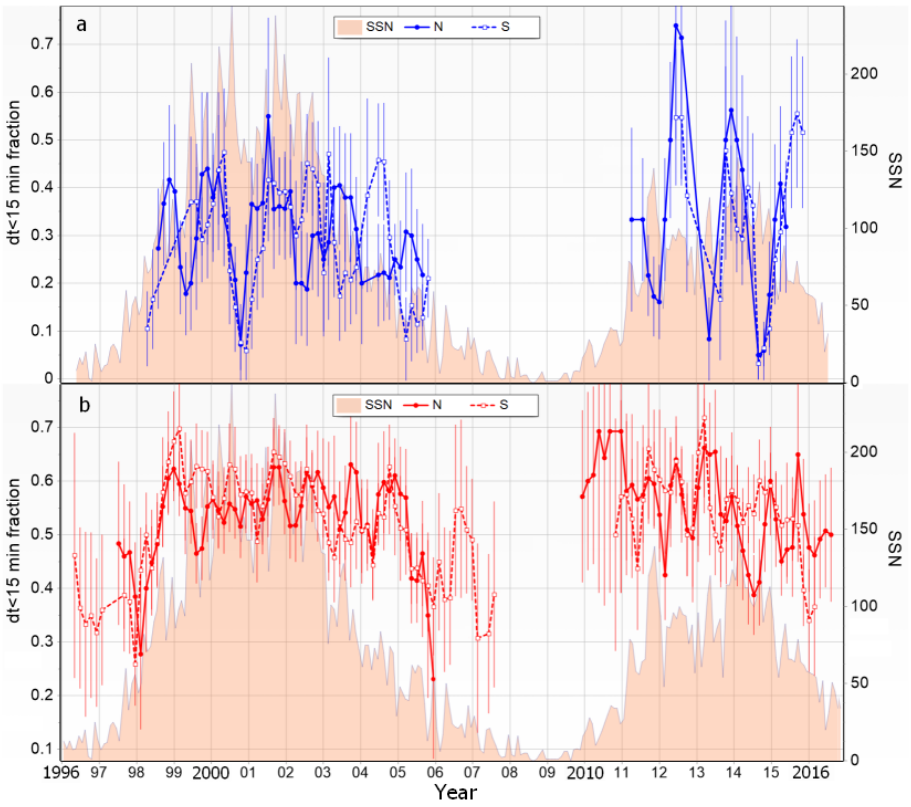

Figure 5. Fraction of SDEs (*solid lines*) with duration dt <15 minutes and LDEs (*dashed lines*) with dt >30 minutes among the ≥M1.0- (a) and C-class (b) flares in Cycles 23 and 24.

trends of the average $dt1$-parameter in Cycles 21 – 23. The smallest values of $dt1$ up to 5 – 6 minutes, intrinsic to SDEs, were observed at the beginning of Cycle 21 for C-class flares and at the beginning of Cycle 22 for ≥M1.0-class flares. The largest average $dt1 \approx 20 - 25$ minutes, characteristic of the ≥M1.0-class LDEs, occurred at the declining phase of Cycle 23. In Cycle 24, the average $dt1$-parameter was also large, but somewhat less than in Cycle 23.

Figure 6b allows us again to connect the variations of the average $dt1$-value outlined above with changes of the fraction of the SDE flares with $dt1$ <10 minutes. In separate QBOs, during each cycle and at the transition from one cycle to another, the average rise time increases (decreases) when the fraction of the SDE flares decreases (increases). Moreover, the fraction of the $dt1$ <10 minutes flares displays trends that are opposite to trends of the average $dt1$-parameter visible on Figure 6a, especially during Cycles 21 – 23. One can see that the variations of the SDE fraction of the C- and ≥M1.0-class flares do not always occur synchronously. The relative QBOs amplitude of the SDE flare fraction is larger than that of the average $dt1$, particularly for the ≥M1.0-class flares in Cycles 23 and 24.

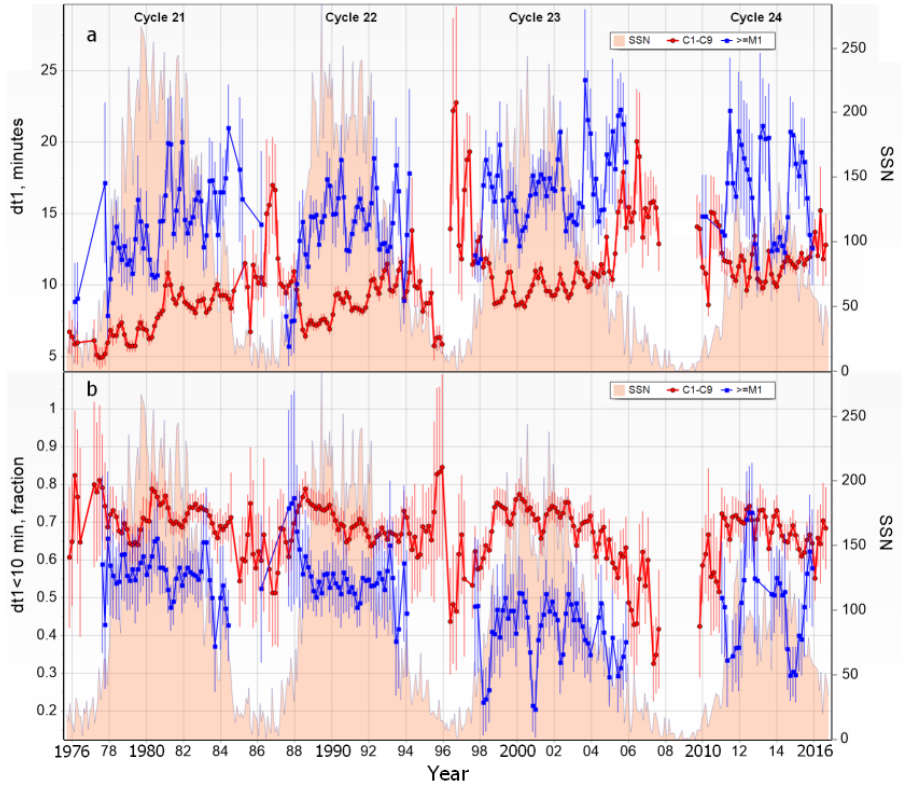

Figure 6. Long-term variations of characteristics of the C-class (*red lines and circles*) and ≥M1.0-class (*blue lines and squares*) flares during 1976 – 2016 against the background of the monthly sunspot number (SSN) in Cycles 21 – 24: (a) the average rise time ($dt1$); (b) fraction of the SDE flares with $dt1 < 10$ minutes.

4. Summary and Discussion

We have presented an analysis of the temporal parameters of the soft X-ray flares registered by the GOES spacecraft during solar Cycles 23 and 24 and additionally in Cycles 21 and 22. We considered the moderate C1.0 – C9.9 class flares and the most intense ≥M1.0-class flares and distinguished among them the impulsive short-duration (SDE) and gradual long-duration (LDE) flares. We focused on parameters (rising, decay times, and duration) and fraction of SDEs and studied the relationship between them and LDEs in the course of these cycles. Our main results can be summarized as follows:

- The fraction of the SDE ≥M1.0-class flares (including spikes) in the weaker Cycle 24 exceeds that in Cycle 23 for all three temporal parameters at the maximum phase and for the decay parameter in the ascending cycle phase. However, Cycles 23 and 24 differ very little in fraction of the SDE C-class flares.
- The temporal parameters of the SDE flares, their fraction, and, consequently, the relationship between SDEs and LDEs do not remain constant,

but they reveal regular antiphased changes within individual cycles and during the transition from one cycle to another.

- At all phases of the four cycles, these changes are characterized by pronounced, large-amplitude quasi-biennial oscillations (QBOs). In different cycles and at the separate phases of individual cycles, such QBOs are superimposed on various systematic trends displayed by the analyzed temporal flare parameters.
- The QBO amplitude and general variability of the intense ≥M1.0-class flares almost always markedly exceed those of the moderate C-class flares.
- The fraction of the SDE ≥M1.0-class flares from the N- and S- hemispheres displays the most pronounced synchronous QBOs in Cycle 24.
- Taken together, these findings mean that ordered long- and medium-term variations of the flare type, *i.e.* alternate transitions from the dominating SDE flares to mainly LDEs, occur during the solar cycle. It is important to emphasize that these variations are not only quantitative but also qualitative in nature.

As noted in the Introduction (see Kahler, 1977; Pallavicini, Serio, and Vaiana, 1977; Ohki *et al.*, 1983; Švestka, 1989), LDEs are associated with the presence of large CMEs and the long-duration post-eruptive energy release that they cause, spanning practically the entire magnetosphere over an AR. As opposed to LDEs, the SDE flares are generated in isolated compact sources as a result of the local reconnection of small-scale magnetic structures (loops) located very low over active regions. This gives us reason to assume that the SDE flares are associated with small sunspots, including those in large groups.

The variations in the character of the flares found by us appear to correspond to the concept that small and large sunspots form two physically distinct populations and behave differently during cycles (Nagovitsyn, Pevtsov, and Livingston, 2012; Nagovitsyn and Pevtsov, 2016; Nagovitsyn *et al.*, 2016). According to these authors, the fraction of the smallest and largest spots changes during the solar cycles in a systematic antiphased way: when the number of small sunspots increases, the number of large spots decreases and *vice versa*. The relationship between the SDE and LDE flares behaves in a similar way. In particular, the that the fraction of SDEs turned out to be markedly increased at the beginning of Cycle 24 may be due to the fact that the proportion of small spots also increased in 2010 – 2011 (*cf.* our Figure 3 and Figure 5 in Nagovitsyn, Pevtsov, and Livingston, 2012).

As for QBOs, these medium-term variations are known to be displayed by various solar and interplanetary proxies indicating their relation with the global solar dynamo mechanism (see Bazilevskaya *et al.*, 2014; Broomhall and Nakariakov, 2015; Barlyaeva *et al.*, 2017 and references therein). In our case, pronounced QBOs are detected in the temporal parameters and fraction of the SDE and LDE soft X-ray flares. These flare QBOs differ from QBOs of other proxies by a number of peculiarities. Their amplitude is so large (especially for the most intense ≥M1.0-class flares) that their detection does not require any spectral analysis. Also, the flare QBO amplitude does not intensify around the cycle

maxima but remains almost unchanged and significant throughout the whole cycles. In addition, these QBOs occur quasi-synchronously in the northern and southern hemispheres of the Sun, particularly for the ≥M1.0-class flares in Cycle 24.

The assumed connection of the regular variations of the flare character in the course of the solar cycles, mainly in the form of the large-amplitude QBOs, with the differing populations of small and large sunspots has reasonable grounds. Many researchers argued that there are two different dynamo processes that act in the deep and near-surface layers of the convective zone and are responsible for the 11-year cycle and more short-term variations of various phenomena of solar activity (see Benevolenskaya, 1998; Brandenburg, 2005; Fletcher *et al.*, 2010; Popova and Yukhina, 2013; Obridko and Badalyan, 2014; Beaudoin *et al.*, 2016). In the context of our results, it is promising to explore the variations of small and large sunspots using the same approach as in the present work, i.e. averaging their number within the running windows of ±2.5 Carrington rotations with a step of two rotations. Such advancement of the analysis of Nagovitsyn, Pevtsov, and Livingston (2012) would allow a detailed comparison of the temporal course of the SDE/LDE flares and small/large sunspots.

The detected variations of the soft X-ray flare type over the solar cycles gives reasons to expect that similar regular transitions between the short- and long-duration flares can occur also in the microwave and hard X-ray ranges. This should also be a subject of further studies.

Acknowledgments We are grateful to the anonymous reviewer for the careful consideration of our article. The authors thank the NOAA/SWPC GOES and SOHO/EIT teams for the open data used in our study. SOHO is a project of international cooperation between ESA and NASA. We are grateful to V.V. Grechnev and V.N. Obridko for useful discussions. This research was partially supported by the Russian Foundation of Basic Research under grants 17-02-00308 and 17-02-00508.

Disclosure of Potential Conflicts of Interest The authors have no conflicts of interest.

References

Barlyaeva, T., Wojak, J., Lamy, P., Boclet, B., Toth, I.: 2017, *J. Atmos. Solar-Terr. Phys.* in press, arXiv.

Bazilevskaya, G., Broomhall, A.-M., Elsworth, Y., Nakariakov, V.M.: 2014, *Space Sci. Rev.* **186**, 359. DOI.

Beaudoin, P., Simard, C., Cossette, J.-F., Charbonneau, P.: 2016, *Astrophys. J.* **826**, 138. DOI.

Belov, A., Garcia, H., Kurt, V., Mavromichalaki, H., Gerontidou, M.: 2005, *Solar Phys.* **229**, 135. DOI.

Benevolenskaya, E.E.: 1998, *Astrophys. J.* **509**, L49. DOI.

Bornmann, P.L., Speich, D., Hirman, J., Pizzo, V.J., Grubb, R., Balch, C., Heckman, G.: 1996, *Proc. SPIE.* **2812**, 309.

Brandenburg, A.: 2005, *Astrophys. J.* **625**, 539. DOI.

Broomhall, A.-M., Nakariakov, V.M.: 2015, *Solar Phys.* **290**, 3095. DOI.

Fletcher, L., Dennis, B.R., Hudson, H.S., Krucker, S., Phillips, K., Veronig, A., Battaglia, M., Bone, L., Caspi, A., Chen, Q., Gallagher, P., Grigis, P.T., Ji, H., Liu, W., Milligan, R.O., Temmer, M.: 2011, *Space Sci. Rev.* **159**, 19. DOI.

Fletcher, S.T., Broomhall, A.-M., Salabert, D., Basu, S., Chaplin, W.J., Elsworth, Y., Garcia, R.A., New, R.: 2010, *Astrophys. J. Lett.* **718**, L19. DOI.
Hathaway, D.H.: 2015, *Living Rev. Sol. Phys.* **12**, 4. DOI.
Janvier, M., Aulanier, G., Démoulin, P.: 2015, *Solar Phys.* **290**, 3425. DOI.
Kahler, S.: 1977, *Astrophys. J.* **214**, 891. DOI.
Nagovitsyn, Y.A., Pevtsov, A.A., Livingston, W.C.: 2012, *Astrophys. J.* **758**, L20. DOI.
Nagovitsyn, Y.A., Pevtsov, A.A.: 2016, *Astrophys. J.* **833**, 94. DOI.
Nagovitsyn, Y.A., Pevtsov, A.A., Osipova, A.A., Tlatov, A.G., Miletskii, E.V., Nagovitsyna, E.Y.: 2016, *Astron. Lett.* **42**, 703. DOI.
Obridko, V.N., Badalyan, O.G.: 2014, *Astron. Rep.* **58**, 936. DOI.
Ohki, K., Takakura, T., Tsuneta, S., Nitta, N.: 1983, *Solar Phys.* **86**, 301. DOI.
Pallavicini, R., Serio, S., Vaiana, G.S.: 1977, *Astrophys. J.* **216**, 108. DOI.
Popova, E.P., Yukhina, N.A.: 2013, *Astron. Lett.* **39**, 729. DOI.
Rieger, E., Kanbach, G., Reppin, C., Share, G.H., Forrest, D.J., Chupp, E.L.: 1984, *Nature* **312**, 623. DOI.
Švestka, Z.: 1989, *Solar Phys.* **121**, 399. DOI.
Tomczak, M., Dubieniecki, P.: 2015, *Solar Phys.* **290**, 3611. DOI.
Zuccarello, F.P., Chandra, R., Schmieder, B., Aulanier, G., Joshi, R.: 2017, *Astron. Astrophys.* **601**, id.A26. DOI.